Virology **258,** 128–140 (1999)
Article ID viro.1999.9702, available online at http://www.idealibrary.com on IDEAL®

Absence of Lung Immunopathology Following Respiratory Syncytial Virus (RSV) Challenge in Mice Immunized with a Recombinant RSV G Protein Fragment

Hélène Plotnicky-Gilquin,[1] Thierry Huss, Jean-Pierre Aubry, Jean-François Haeuw, Alain Beck, Jean-Yves Bonnefoy, Thien Ngoc Nguyen, and Ultan F. Power[1]

Centre d'Immunologie Pierre-Fabre, 5, Avenue Napoléon III, 74 164, St. Julien en Genevois, France

Received January 8, 1999; returned to author for revision February 3, 1999; accepted March 11, 1999

The relative immunopathogenic potential of a recombinant fusion protein incorporating residues 130–230 of respiratory syncytial virus (RSV-A) G protein (BBG2Na), formalin-inactivated RSV-A (FI-RSV), and phosphate-buffered saline (PBS) was investigated in mice after immunization and RSV challenge. FI-RSV priming resulted in massive infiltration of B cells and activated $CD4^+$ and $CD8^+$ T lymphocytes in mediastinal lymph nodes (MLN) and lungs, where eosinophilia and elevated IFN-γ, IL-2, -4, -5, -10, and -13 mRNA transcripts were also detected. PBS-primed mice showed only elevated pulmonary IL-2 and IFN-γ mRNAs, while an activated $CD8^+$ T cell peak was detected in MLN and lungs. Cell infiltration also occurred in MLN of BBG2Na-immunized mice. However, there was no evidence of T cell, B cell, or granulocyte infiltration or activation in lungs, while transient transcription of Th1-type cytokine genes was evident. The absence of pulmonary infiltration is unlikely due to insufficient viral antigen. Thus, this recombinant fusion RSV G fragment does not prime for adverse pulmonary immunopathologic responses. © 1999 Academic Press

INTRODUCTION

Respiratory syncytial virus (RSV) is a major respiratory pathogen responsible for severe pulmonary disease in very young children, immunodeficient patients, and the elderly (Collins *et al.,* 1996). First infection generally occurs despite the presence of maternal antibodies and represents the most common cause of infant hospitalization. Furthermore, antiviral immunity is poorly induced and reinfections are frequent throughout life.

Despite the clinical and economic importance of this infection, efforts to develop an efficacious RSV vaccine have been unsuccessful to date (Anderson and Heilman, 1995). Live attenuated, inactivated, and subunit vaccine candidates failed to protect and/or demonstrated potential to enhance lung pathology upon subsequent RSV infection (for review see Murphy *et al.,* 1994). Indeed, RSV-enhanced disease was first encountered in the 1960s during the clinical evaluation of a formalin-inactivated whole RSV preparation (FI-RSV). This vaccine preparation not only failed to protect the immunized children but also enhanced the rate of hospitalization after subsequent RSV infection and was associated with two deaths (Kim *et al.,* 1969).

Mice and cotton rats are semipermissive to RSV infection and also show enhanced pathology upon RSV challenge following immunization with FI-RSV (Prince *et al.,* 1986; Vaux-Peretz *et al.,* 1992). In these animal models, RSV major surface glycoproteins F (implicated in viral fusion and syncytium formation) and G (attachment protein) are the principal protagonists of protective immune responses (Connors *et al.,* 1991; Routledge *et al.,* 1988). In contrast to the F protein, G protein is characterized by a particularly high antigenic and genetic variability between and within RSV subgroups (Johnson and Collins, 1988; Cane *et al.,* 1991). This suggests the influence of high environmental and/or immunologic pressure. However, both F and G proteins were implicated in adverse anti-RSV responses. The most severe pulmonary disease, characterized by lymphocyte infiltration and eosinophilia, resulted from prior immunization with G protein and was associated with the induction/recall of a strong Th2-type anti-RSV T cell response upon viral challenge (Vaux-Pertz *et al.,* 1992; Alwan *et al.,* 1994; Murphy *et al.,* 1990; Hancock *et al.,* 1996). These immunological events are also induced in the FI-RSV associated lung pathogenesis (Waris *et al.,* 1996; Connors *et al.,* 1994). Interestingly, the G protein has a unique structure with over 50% of its molecular weight estimated to be carbohydrate, the majority of which is O-linked sugars (Wertz *et al.,* 1985). It was hypothesized that this exceptional rate of glycosylation may play a role in the induction of a Th2-type response and may account for the immunopathologic potential of this protein (Anderson and Heilman, 1995).

Recently, we evaluated the protective efficacy of an RSV G protein fragment (G2Na), which is produced in *Escherichia coli* as a recombinant fusion protein (BBG2Na). BBG2Na comprises residues 130–230 of RSV-A G protein (G2Na) fused to BB, an albumin binding

[1] To whom correspondence and reprint requests should be addressed. Fax: (33) 450.35.35.90. E-mail: helene.plotnicky@pierre-fabre.com; ultan.power@pierre-fabre.com.

0042-6822/99 $30.00

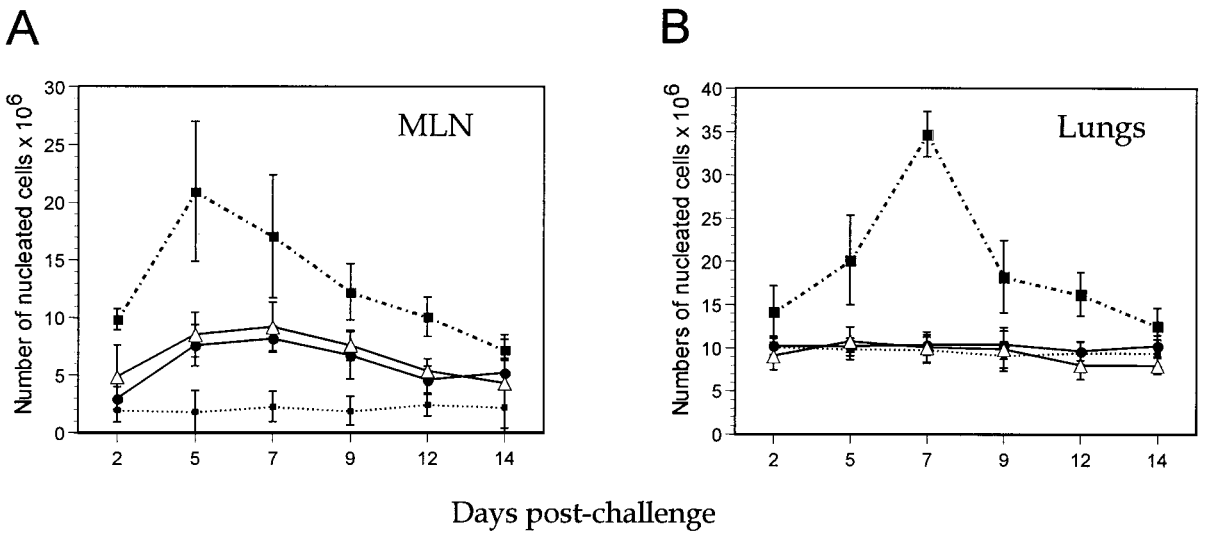

FIG. 1. Nucleated cell infiltration in MLN and lungs following RSV challenge. BALB/c mice were immunized three times i.p. with PBS (—△—), BBG2Na (—●—), or FI-RSV (–·■–·) in Alhydrogel and challenged i.n. with RSV-A. They were sacrificed from day 2 to day 14 thereafter. Nucleated cells were isolated from MLN and lungs, enumerated, and compared to cells from naive unchallenged mice (···■···). Mean values ± SD of numbers of nucleated cells in MLN (A) and lungs (B) were calculated from groups of 5 to 12 mice for each time point.

domain of streptococcal protein G with carrier protein-related properties (Libon *et al.,* 1999; Makrides *et al.,* 1996; Nygren *et al.,* 1991). G2Na includes a conserved subgroup A-specific protective epitope (residues 174–187) (Trudel *et al.,* 1991) and a stretch of amino acid residues that are completely conserved in all known human RSV isolates (residues 164–176) (Collins *et al.,* 1996). Accordingly, BBG2Na was shown to induce high levels of antibodies in mice reactive with prototype subgroup A and B RSV strains, as well as a rapid, potent, and long-lasting protection against RSV-A infection. In addition, protective efficacy was also demonstrated in cotton rats against both RSV-A and -B (Power *et al.,* 1997).

A previous evaluation of serum cytokine profiles in mice demonstrated that although BBG2Na induces a predominant Th2-type T cell response upon immunization, no production of IL-4, IL-5, or IgE is detected after live RSV challenge. Thus, the Th2-type memory T cells are not recalled in the periphery following challenge (Corvaia *et al.,* 1997). The aim of the current study was to investigate the effect of RSV challenge in the lower respiratory tract of BBG2Na-immunized mice. For this purpose, we analyzed the fine cellular and molecular events occurring in mediastinal lymph nodes (MLN) and lung tissues after RSV-A challenge. Our data clearly demonstrate that, in contrast to FI-RSV, this recombinant RSV G protein fragment does not prime for Th2-type RSV immunopathologic responses.

RESULTS

Effects of priming and RSV challenge on nucleated cell infiltration in MLN and lungs

To determine the comparative effects of priming with various antigens on postchallenge cellular responses, the kinetics of nucleated cell populations infiltrating MLN and lung tissues of BBG2Na-, PBS-, and FI-RSV-immunized mice were analyzed after intranasal (i.n.) challenge with 10^5 $TCID_{50}$ RSV-A. The numbers of nucleated cells increased rapidly from day 2 postchallenge in the MLN and lungs of FI-RSV-immunized mice and peaked at day 5 for MLN and at day 7 for lungs, with mean cell numbers of 21 ± 6.1 × 10^6 and 34.7 ± 2.6 × 10^6, respectively (Figs. 1A and 1B). Extensive and comparable cell infiltration postchallenge was evident in PBS- and BBG2Na-immunized mice in the MLN compared with naive unchallenged mice (approximately 8 × 10^6 and 2 × 10^6, respectively), but not in the lungs. However, this MLN infiltration was significantly reduced relative to the FI-RSV-primed mice.

Flow cytometric analysis of the isolated cells based on their forward- and side-scatter distribution demonstrated that lymphocytes constituted the principal nucleated cell population present in MLN of all groups and in the lungs of naive unchallenged mice (not shown). This was also the case for BBG2Na- and PBS-immunized mice after RSV-A challenge. In contrast, a significant population of large granular cells was also evident in the lungs of mice immunized with FI-RSV, representing 30 to 50% of the nucleated cell lung infiltrate between days 5 and 9 postchallenge (not shown). Sorting of cells in the large granular cell gate from six or seven animals per group, followed by May-Grünwald Giemsa staining and light microscopic examination, revealed that the recovered cells comprised 63 ± 7% eosinophils in FI-RSV-immunized/challenged mice, compared with less than 8% in the other groups. The total number of eosinophils infiltrating the lungs was subsequently extrapolated as a function of the total number of nucleated cells isolated

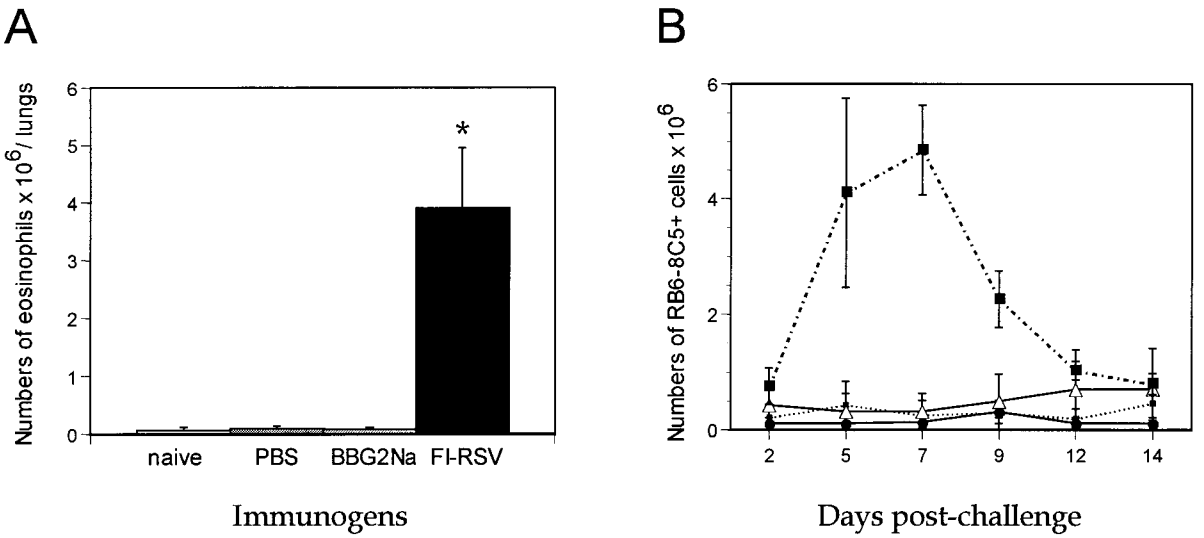

FIG. 2. Infiltration of granulocyte cells in lung tissues of FI-RSV-immunized mice after RSV-A infection. Mice were immunized three times i.p. with PBS (—△—), BBG2Na (—●—), or FI-RSV (– · ■– ·) in Alhydrogel and challenged i.n. with RSV-A. Infiltrating cells were isolated upon enzymatic digestion of the lung tissues and enumerated. (A) Large granular cells were sorted by FACS. The percentage of eosinophils was determined by light microscopy after staining with May-Grünwald Giemsa and extrapolated to total numbers as a function of total nucleated infiltrating cell counts. Mean numbers of eosinophils ± SD were calculated for groups of 6 to 8 mice. $*P < 0.05$ calculated by *t* test using null hypothesis. (B) Lung infiltrating cells isolated from days 2 to 14 postchallenge were stained with antibody RB6-8C5 and analyzed by flow cytometry after dead cells and debris were eliminated by gating on forward and side scatter. The percentage of stained cells was extrapolated to total numbers as indicated above. Mean total numbers of granulocyte cells ± SD were calculated for groups of 5 to 11 animals for each time point and compared with those from 10 naive unchallenged mice per time point (· · ·■· · ·).

from the corresponding lungs. As represented in Fig. 2A, significant lung eosinophilia was observed in the FI-RSV-A-immunized/RSV-A-challenged group, but not in the other groups.

Consistent with these data, the number of lung RB6-8C5$^+$ cells (granulocytes) at day 5 postchallenge was 20 to 30 times higher in the FI-RSV animals than in the other groups (Fig. 2B). This population peaked at day 7 and could still be detected at day 14 in some animals. In comparison, and in agreement with previous histologic studies of mouse lungs undergoing primary RSV infection (Anderson *et al.,* 1990), PBS-immunized animals demonstrated a small increase in RB6-8C5$^+$ cells at late time points postchallenge (days 12 and 14). No modification was observed in the BBG2Na group, even after a challenge dose of 10^6 $TCID_{50}$ of RSV-A (not shown), in which granulocyte populations always remained similar to those of naive unchallenged mice.

Effects of priming and RSV challenge on lymphocyte populations

Both B (CD45R-B220$^+$) and T (CD4$^+$ and CD8$^+$) lymphocytes were significantly increased postchallenge in MLN and lungs of mice immunized with FI-RSV (Figs. 3, 4, and 5). At the peak of cell infiltration (days 5 and 7 postchallenge), B and T lymphocyte populations in the MLN were more than 4 and 2 times more numerous, respectively, than in the other groups (Figs. 3A, 4A, and 4C, $P < 0.05$). In the MLN of FI-RSV-primed mice, expression of early activation marker CD69 increased rapidly on CD4$^+$ and CD8$^+$ T cells and was maintained for at least 14 days postchallenge (Figs. 4B and 4D), indicating the induction of a strong cellular response of both these T lymphocyte subsets after RSV challenge. Activation of T cells was also observed in MLN of the PBS group but it was restricted to CD8$^+$ T cells at early time points. In contrast, although total numbers of CD45RB220$^+$, CD4$^+$, and CD8$^+$ cells increased in BBG2Na-immunized mice in a manner comparable to the PBS group (Figs. 3A, 4A, and 4C), there was no evidence of T cell activation in the MLN (Figs. 4B and 4D), suggesting that RSV challenge in this group stimulated only a B cell response.

As evident in the MLN, intense B and T cell infiltration and activation occurred in the lungs of FI-RSV-immunized/challenged mice (Figs. 3B and 5). CD4$^+$ and CD8$^+$ T cells were two and five times as numerous, respectively, as in the lungs of naive unchallenged mice. More than 95% of the cells were TCR$\alpha\beta^+$ (data not shown), concordant with the phenotype of pulmonary T cells induced by RSV infection (Openshaw, 1991). Increased expression of CD69 was evident for more than 30% of the CD4$^+$ and CD8$^+$ cells on days 7 and 9, respectively (Figs. 5B and 5D). A similar percentage of CD69hi$^+$ CD8$^+$ T cells was also observed in the PBS group at day 5, consistent with the MLN data and confirming the

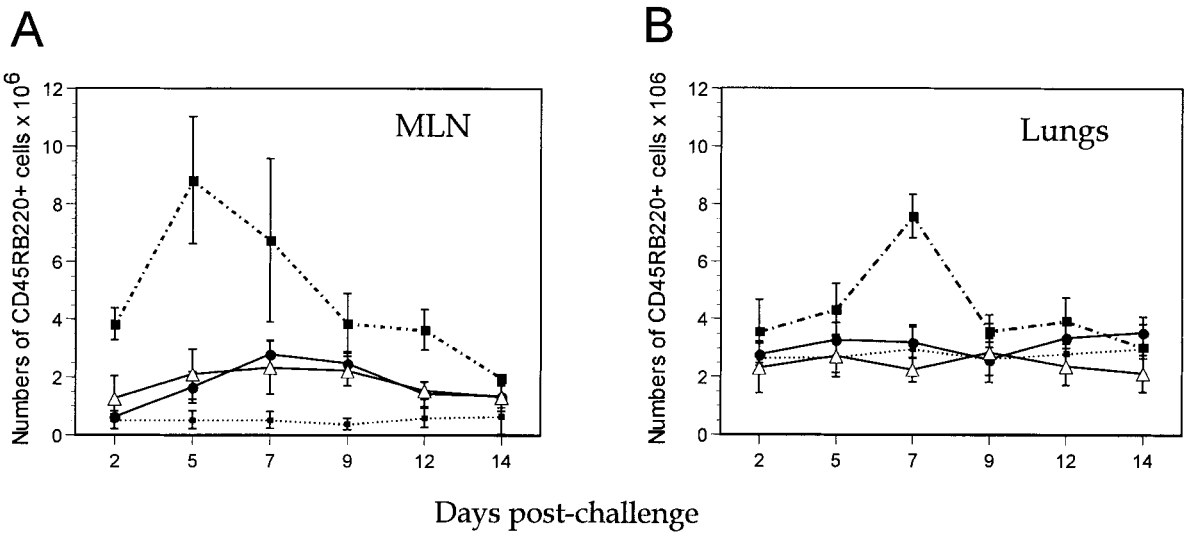

FIG. 3. Kinetics of B cell infiltration in MLN and lungs after RSV challenge. Mice were immunized three times i.p. with PBS (—△—), BBG2Na (—●—), or FI-RSV (–·■–·) in Alhydrogel and challenged i.n. with RSV-A. Infiltrating cells from MLN and lung tissues were enumerated, stained with anti-CD45RB220 antibody, and analyzed by flow cytometry after gating on forward and side scatter. Mean total numbers of B cells ± SD in MLN (A) and lungs (B) were calculated from groups of 5 to 12 mice for each time point and compared with those from 7–8 naive unchallenged mice per time point (···■··).

induction of a strong $CD8^+$ T cell response. Furthermore, consistent with previous observations (Anderson *et al.,* 1990; Taylor *et al.,* 1985), a significant increase in the total number of pulmonary $CD8^+$ T cells was evident in the latter group on days 7 and 9 postchallenge compared with naive unchallenged controls (Fig. 5C, $P < 0.05$). Interestingly, 5 to 10% of $CD4^+$ T cells from PBS immunized mice were also activated, indicating that RSV-A infection induced a local, albeit relatively low, $CD4^+$ T cell response. These patterns of T lymphocyte activation were confirmed by the enhanced expression of LFA-1 (data not shown).

No such increase or activation in lymphocyte subsets was detected in pulmonary infiltrating cells of BBG2Na-immunized mice. The ratios of total numbers of $CD4^+CD69hi^+$ to $CD8^+CD69hi^+$ cells in these mice remained comparable to those of naive unchallenged controls during the 2 weeks following RSV-A challenge (approximately 2:1). These ratios were reduced in PBS-immunized mice (1:1.5), reflecting the predominance of activated $CD8^+$ T cells. In contrast, they were approximately 10 times greater (23:1, $P < 0.05$) in the FI-RSV group in which activated $CD4^+$ T cells were strikingly predominant at day 5 compared with activated $CD8^+$ T cells. Thus, these data clearly demonstrate the absence of immunopathologic T cell responses in lung tissues of BBG2Na-immunized mice, in stark contrast to FI-RSV-immunized animals.

Effects of priming and RSV challenge on cytokine mRNA profiles

A characteristic Th2-type cytokine profile was previously demonstrated in FI-RSV-immunized mice undergoing an immunopathologic reaction to RSV challenge, while a primary anti-RSV response was associated mainly with the Th1-type cytokine profile (Graham *et al.,* 1993; Hussell *et al.,* 1996). We therefore determined whether the massive eosinophil and lymphocyte infiltration observed in lungs of FI-RSV-immunized/challenged mice, in contrast to BBG2Na-immunized/challenged mice, also reflected major differences in the cytokine expression among the various groups. For this purpose, we assessed representative Th1 and Th2 cytokine mRNA changes upon RSV-A challenge in pulmonary lymphocytes by a sensitive and specific semiquantitative RT-PCR ELISA technique (Janezic *et al.,* 1995). The data are presented as the ratio of the OD_{405nm} for the cytokine mRNA relative to the OD_{405nm} for β-actin mRNA.

The primary anti-RSV response developed in PBS-immunized animals was associated with increased expression of IL-2 and INF-γ mRNA (Figs. 6A and 6B). Messenger RNA levels for these Th1-type cytokines peaked at day 5, being 6 and 11.5 times greater, respectively, than levels in naive unchallenged controls ($P < 0.05$). Subsequently, the levels decreased progressively until day 14 postchallenge. The postchallenge kinetics of IL-2 mRNA expression in lung infiltrating cells from BBG2Na- and PBS-immunized mice paralleled one another during the first week, although the latter group demonstrated slightly higher levels. These results are consistent with a Th1-type cellular response in the lungs of the implicated mice (Hussell *et al.,* 1996). However, at later time points, mean IL-2 mRNA expression in BBG2Na-immunized mice decreased to baseline levels observed in naive unchallenged mice. In lung infiltrating

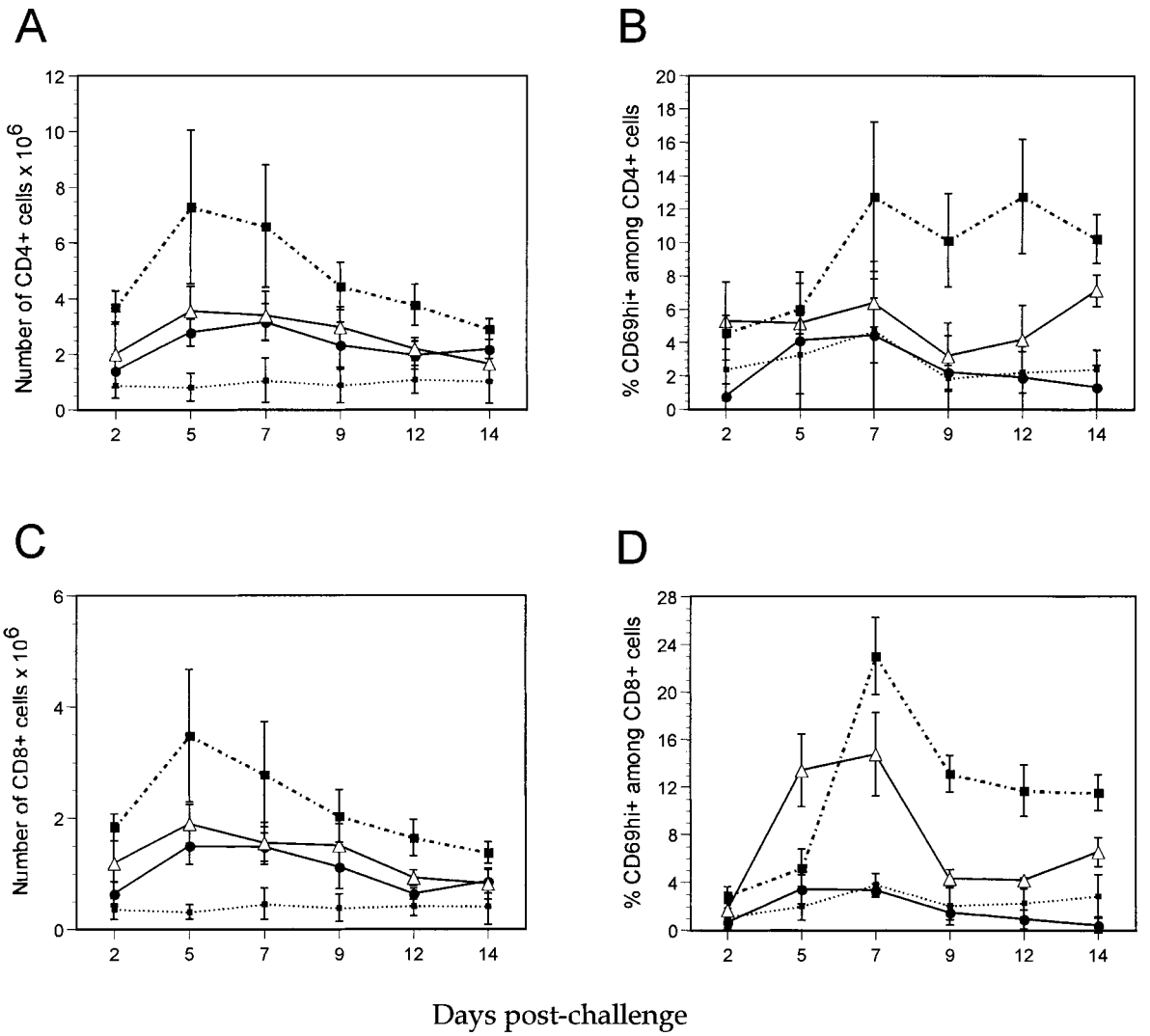

FIG. 4. Activated CD4 and CD8 T lymphocytes in MLN of mice after RSV challenge. Mice were immunized three times i.p. with PBS (—△—), BBG2Na (—●—), or FI-RSV (– • ■– •) in Alhydrogel and challenged i.n. with RSV-A. Infiltrating cells from MLN were enumerated, stained with fluorescent antibody combinations specific for CD4, CD8, and CD69, and analyzed by flow cytometry after gating on forward and side scatter. Mean total numbers of $CD4^+$ (A) and $CD8^+$ (C) and percentages of activated ($CD69hi^+$) CD4 (B) and CD8 (D) T cells ± SD were calculated from groups of 5 to 12 mice for each time point and compared with those from 7–8 naive unchallenged mice per time point (· · ■ · ·).

cells from FI-RSV-immunized animals, IL-2 mRNA accumulated until day 9 postchallenge ($P < 0.05$). IFN-γ mRNA levels in BBG2Na-immunized mouse lung cell infiltrates were never statistically different from those of naive mice. In contrast, they were strongly enhanced by day 5 in infiltrating cells from both PBS- and FI-RSV-immunized mice. Unlike PBS-immunized mice, however, IFN-γ mRNA levels in the latter mice remained stable during the following 9 days ($P < 0.05$).

For Th2-type cytokines, including IL-4, IL-5, IL-10, and IL-13, markedly elevated levels of mRNA were observed almost exclusively in the lung infiltrating cells of FI-RSV-immunized animals (Figs. 6C, 6D, 6E, and 6F). Mean IL-4 and IL-13 mRNA levels peaked at day 5 ($P < 0.05$), being 20 and 60 times higher than those measured in any other group. Elevated IL-5 and IL-10 mRNA expression was already evident at day 2 postchallenge (being 15 and 10 times higher, respectively, than those of any other group, $P < 0.05$) and remained stable until day 5. Subsequently, mRNA expression gradually diminished, such that by day 14, levels close to baseline were observed for all Th2-type cytokines. In contrast, only low levels of Th2-type cytokine mRNAs were detected in the BBG2Na and PBS groups, which were in general similar to cytokine expression levels in the lungs of naive unchallenged mice. One exception was the appearance of a peak of IL-10 at day 9 postchallenge in PBS-immunized mice (Fig. 6E, $P < 0.05$). Slightly elevated IL-4 and IL-13 mRNA expression was also observed on day 5 in these animals but was not statistically different from expression in naive mice. These data are consistent with

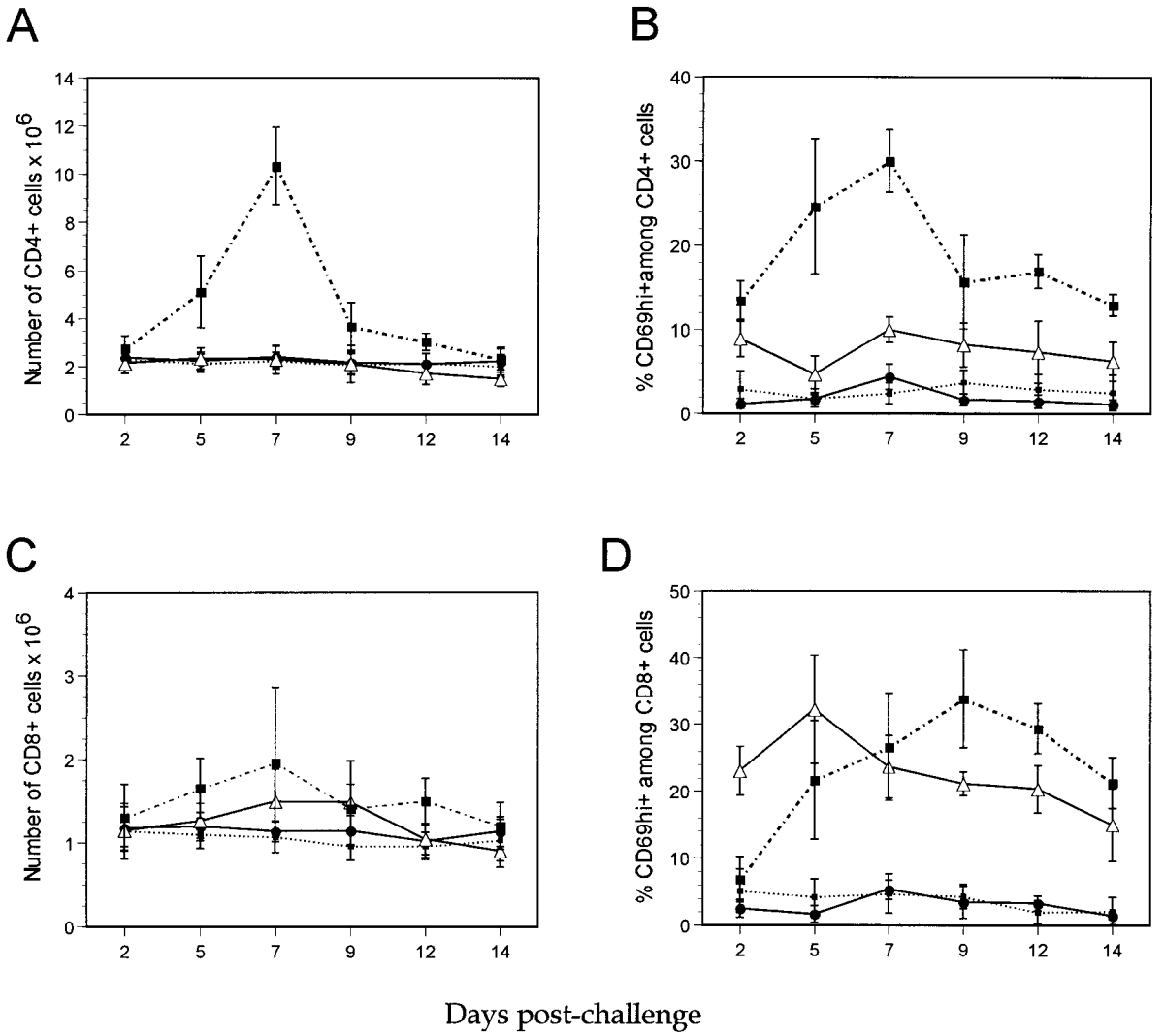

FIG. 5. Activated CD4 and CD8 T lymphocytes in lung tissues of mice after RSV challenge. Mice were immunized three times i.p. with PBS (—△—), BBG2Na (—●—), or FI-RSV (–·■–·) in Alhydrogel and challenged i.n. with RSV-A. Infiltrating cells from lung tissues were enumerated, stained with fluorescent antibody combinations specific for CD4, CD8, and CD69, and analyzed by flow cytometry after gating on forward and side scatter. Mean total numbers of $CD4^+$ (A) and $CD8^+$ (C) and percentages of activated ($CD69hi^+$) CD4 (B) and CD8 (D) T cells ± SD were calculated from groups of 5 to 12 mice for each time point and compared with those from 7–8 naive unchallenged mice per time point (···■···).

the lung cell infiltration kinetics reported above. Furthermore, they confirm that, in contrast to FI-RSV, Th2-type pulmonary immunopathologic responses do not occur upon live viral challenge of BBG2Na-primed mice.

Effects of immunization on the presence of viral mRNA transcripts

Previous work from our laboratory demonstrated that at 24 h following intranasal RSV challenge, no or minimal detectable tissue culture infectious virus could be found in lungs of mice immunized three times with 20 μg BBG2Na (Power *et al.,* 1997). Therefore, the possibility existed that the rapid sterilizing protective efficacy of BBG2Na may be responsible for the absence of enhanced immunopathology upon RSV-A challenge. The persistence of viral transcripts in the absence of detectable infectious virions was previously demonstrated in RSV and vesicular stomatitis virus animal models (Barrera and Letchworth, 1996; Hegele *et al.,* 1994). Thus, we analyzed RSV G mRNA transcripts by RT-PCR ELISA in the lungs of BBG2Na-, FI-RSV-, and PBS-immunized mice 2 days after challenge. Not surprisingly, high virus-specific mRNA levels were detected in lung tissues of PBS-immunized mice, indicating the occurrence of viral transcription in the pulmonary tissues (Fig. 7). Viral mRNA was also detected in lung tissues from BBG2Na- and FI-RSV-immunized animals, albeit at lower levels. Average mRNA levels were much lower in the lungs of FI-RSV- than of BBG2Na-immunized animals ($P < 0.05$), indi-

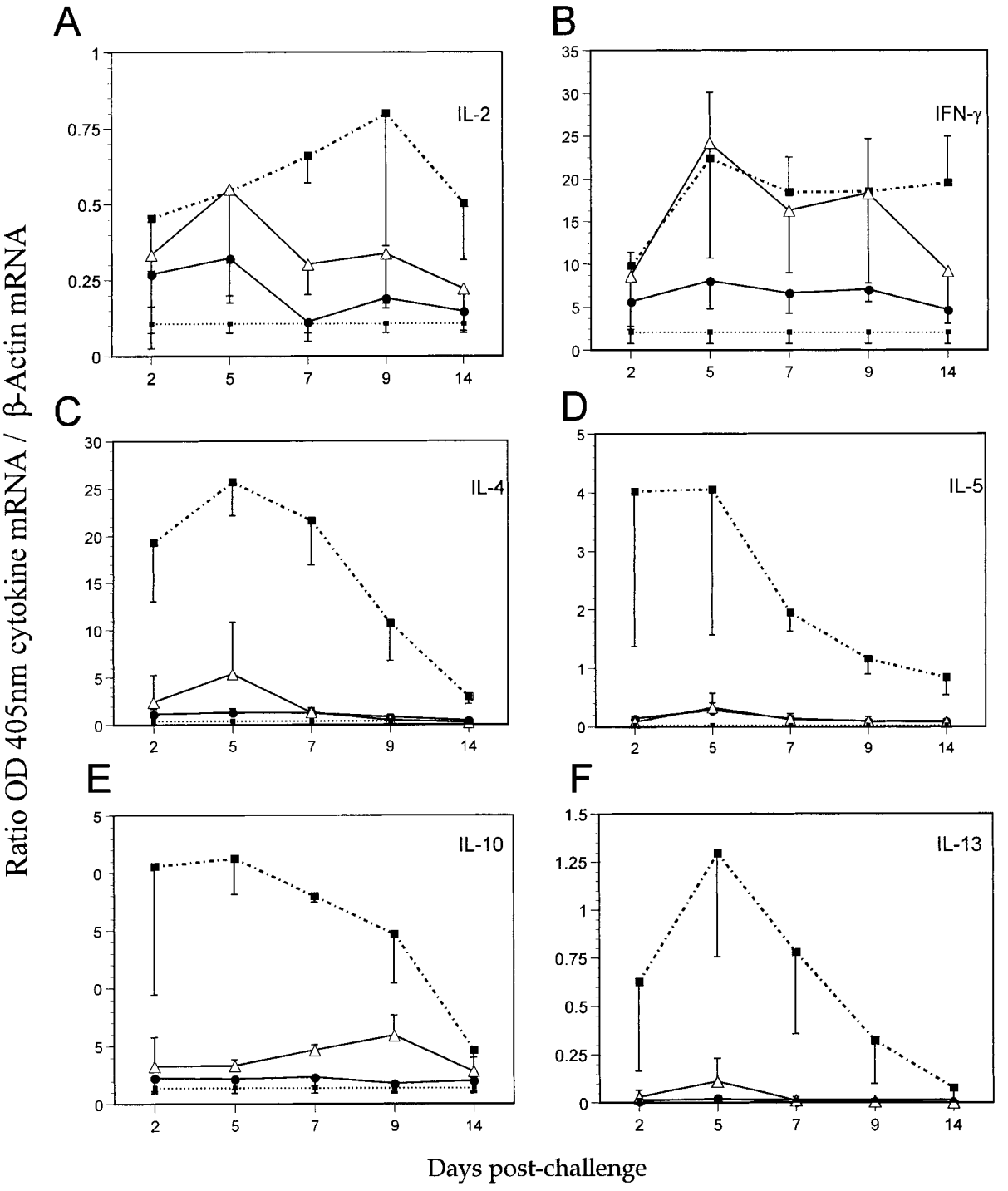

FIG. 6. Kinetics of Th1 (A, B) and Th2 (C, D, E, F) cytokine mRNA expression in lung infiltrating cells upon RSV challenge. Groups of four to seven mice for each time point were immunized with BBG2Na (—●—), FI-RSV (–·■–·), or PBS (—△—) three times in Alhydrogel. Ten days after the last immunization, mice were challenged with RSV-A. On days 2, 5, 7, 9, and 14 postchallenge, lung infiltrating cells were isolated, and total mRNA was extracted and reverse-transcribed into cDNA. PCR amplified products were analyzed by semiquantitative ELISA. OD_{405nm} ratios of cytokines to β-actin-amplified products were calculated and results shown are means ± SD of OD_{405nm} ratios. Naive unchallenged mice were used to determine baseline levels for each cytokine (···■···).

cating that clearance of virus was in fact most effective in the former mice. Therefore, as the low level of virus gene transcription following challenge in the lungs of FI-RSV-primed mice seemed to be sufficient to recall immunopathologic responses in these animals, the absence of immunopathology in BBG2Na-immunized mice is unlikely to be explained by a higher sterilizing protection than in the FI-RSV group.

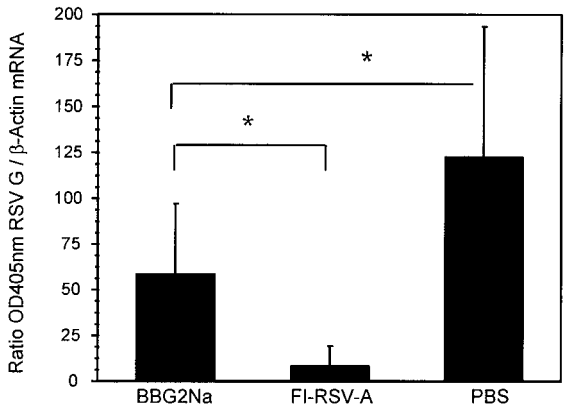

FIG. 7. Effects of BBG2Na, FI-RSV, and PBS immunizations on viral gene expression in lung tissues 2 days postchallenge with RSV. The presence of viral G mRNA in mouse lungs was analyzed by RT-PCR ELISA, as outlined under Materials and Methods. Results calculated from five or six animals per group represent the means ± SD of OD_{405nm} for the G mRNA relative to the OD_{405nm} for the β-actin mRNA. *$P < 0.05$ calculated by the *t* test using null hypothesis.

DISCUSSION

Major obstacles to vaccine development against RSV infection include induction of partial immunity and/or severe immunopotentiation of RSV disease. In this communication, we demonstrate that a recombinant RSV-A G protein fragment, which is highly immunogenic and protects rodents against prototype RSV A and B viruses (Power *et al.,* 1997), does not prime for deleterious Th2-type anti-RSV pulmonary immunopathologic responses.

In our experiments, the primary anti-RSV immune response in PBS-immunized mice was characterized by a peak of activated $CD8^+$ T cells, which was first evident in the MLN and then in the lungs, the detection of significant levels of pulmonary IL-2 and IFN-γ mRNAs, and the absence of enhanced Th2-type cytokine expression at early time points. These data are indicative of Th1-type responses, which is consistent with previous reports of RSV infection in adult humans and rodents (Graham *et al.,* 1993; Hussell *et al.,* 1996; Anderson *et al.,* 1994). Activated $CD4^+$ T cells were also detected, consistent with their role in the development of both cytotoxic and B lymphocyte immune responses (for review see Swain, 1991). Indeed, these cells may represent the major cellular source of IL-2 mRNA. The detection of a significant peak of IL-10 mRNA at day 9 (consistent with the work of Hussel *et al.,* 1996), a cytokine that represses Th1-type cellular immune responses (Fiorentino *et al.,* 1991), suggests active immunosuppression of the cytotoxic T cell response in these animals.

Alternatively, the postchallenge anti-RSV immunopathologic responses in FI-RSV-immunized mice was characterized by a massive cellular infiltration of all lymphocyte subsets in MLN and a predominance of activated $CD4^+$ T lymphocytes and eosinophils in the lungs. Interestingly, elevated expression of both Th1- (IFN-γ, IL-2) and Th2-type (IL-4, IL-5, IL-10, IL-13) cytokine mRNAs was evident in lung infiltrates isolated from these animals, indicating that memory responses upon RSV challenge were not exclusively Th2 in nature. However, the elevated Th2-type cytokine gene expression was exclusive to the FI-RSV primed mice. This is consistent with mechanistic roles of IL-4, IL-5, and IL-10 in FI-RSV- and G-protein-induced enhanced pathology (Connors *et al.,* 1992, 1994; Hancock *et al.,* 1996). Although absolute levels appeared low, the most striking differences in cytokine expression levels between FI-RSV-immunized mice and the other groups related to IL-13 mRNA synthesis, thereby suggesting a role for IL-13 in FI-RSV induced immunopathology. Elevated expression of IFN-γ and IL-2 mRNAs suggests that these cytokines do not exercise antagonistic roles in preventing enhanced pulmonary immunopathology.

In striking contrast, mice immunized with BBG2Na showed no evidence of Th2-type cytokine mRNA synthesis, T cell activation, cell infiltration, or inflammatory responses in the lungs during the 2 weeks following intranasal challenge. T and B cell infiltration did occur in the MLN but it remained comparable to that of PBS-immunized/challenged mice. However, no activated $CD8^+$ T cells were identified consistent with the inability of RSV G protein to induce a $CD8^+$ cytotoxic T cell response (Johnson and Collins, 1988; Openshaw *et al.,* 1990). These data indicate that BBG2Na priming influences the type of MLN infiltrating responses compared with mice undergoing primary infection. In addition, although their levels were relatively low compared to PBS-immunized/challenged mice, IL-2 and IFN-γ mRNA expression was slightly increased in lung infiltrates during the first week compared to expression in naive unchallenged mice. This is suggestive of a tendency toward a Th1-type response postchallenge in these animals. Overall, our data indicate that Th2-type memory T cells or cytokines were not recalled in lung tissues following RSV challenge of BBG2Na-primed mice. This is concordant with the previously reported cytokine analyses performed in BBG2Na-immunized mice, which demonstrated the absence of IL-4, IL-5, and IgE recall responses in the serum following live viral challenge (Corvaia *et al.,* 1997). Our data are in stark contrast to previous work showing Th2-type RSV immunopathologic response following prior immunization with native or vaccinia virus-expressed RSV G protein (Vaux-Peretz *et al.,* 1992; Alwan *et al.,* 1994; Hancock *et al.,* 1996; Stott *et al.,* 1987). The switch from a predominantly Th2-like response after immunization with BBG2Na toward a discrete Th1-like profile following RSV-A challenge suggests that the virus-induced Th1-like cytokine responses supersede the preexisting BBG2Na-induced profiles. Alternatively, the Th2-like responses induced following FI-RSV or native G protein priming might overwhelm the challenge RSV response.

Recently, an overlapping domain (residues 193–203) and a T cell epitope (residues 184–198), which were shown to be implicated in RSV enhanced pathology, were identified on the G protein (Sparer *et al.,* 1998; Tebbey *et al.,* 1998). This domain and T cell epitope map within the G2Na fragment. However, our data indicate that these elements are insufficient in the context of BBG2Na to induce aberrant cellular infiltration in the lungs postchallenge. Furthermore, in contrast to a previous hypothesis (Graham *et al.,* 1993) suggesting that sterilizing immunity may prevent or diminish the extent of enhanced pathology, we did not find a correlation between the level of viral transcription in the lungs (and by extension the level of viral antigens) and the induction of enhanced pathology. Indeed, our data suggest that BBG2Na-immunized mice had more viral antigen in their lungs than FI-RSV-immunized mice. Therefore, as FI-RSV primed mice demonstrated extensive immunopathology upon challenge, the absence of pathology in the BBG2Na group is unlikely to be due to insufficient viral antigens.

As BBG2Na is produced as a fusion protein in a prokaryotic expression system, several hypotheses may be drawn to explain the absence of RSV enhanced disease in BBG2Na-immunized/challenged mice. First, BBG2Na is nonglycosylated by virtue of its prokaryotic origin, suggesting the possibility that intracellular processing by antigen-presenting cells is altered relative to the native G protein, thereby influencing the type of immune response generated. However, glycosylation does not seem to be a critical factor for the induction of enhanced pathology since significant lung eosinophilia was induced after RSV challenge in mice primed with a synthetic peptide coupled to KLH (Tebbey *et al.,* 1998). Second, the carrier protein properties of BB, coupled with its high affinity for serum albumin and its capacity to extend the *in vivo* half-life of its fusion partner (Makrides *et al.,* 1996; Nygren *et al.,* 1991), suggest the likelihood that G2Na is presented to the immune system in a different manner and with different kinetics than the native G protein. Third, $CD4^+$ T cell clones generated by immunization with BBG2Na might be principally elicited by BB, with fewer T cell clones specific for G2Na. In contrast, immunization with FI-RSV or the native G protein alone is likely to stimulate a greater number of RSV-specific T cell clones, which are recalled after live RSV challenge. Finally, memory T cells induced upon immunization with BBG2Na may fail to recognize the antigens provided by the viral challenge. Indeed, previous experiments showed that, unlike live RSV, BBG2Na administered by the i.n. route in the presence of cholera toxin subunit B stimulated IL-4 and IL-5 secretion in the serum of BBG2Na-immunized mice (Corvaia *et al.,* 1997). Reactivation of Th2-type T cells elicited by immunization with BBG2Na was thus possible but entirely dependent upon appropriate stimulation. This stimulation was evidently not provided by the RSV challenge. These hypotheses are currently under investigation.

Previous studies demonstrated the importance of the priming on the disease-enhancing immune response and indicated that eliciting a Th2-type primary response was critical for the induction of FI-RSV-like immunopathology (Graham *et al.,* 1993; Stott *et al.,* 1987; Waris *et al.,* 1997). Alternatively, our data with Alhydrogel adsorbed BBG2Na clearly indicate that induction of a Th2-type response upon immunization does not necessarily imply Th2-type recall responses and immunopathology upon RSV challenge. This discrepancy opens the possibility of exploiting BBG2Na, in comparison with FI-RSV, to identify correlates of RSV vaccine safety and/or postinfection pulmonary pathology following vaccination, a key requirement for clinical development of such vaccines in seronegative infants. In view of the data presented above and previous reports (Brandt *et al.,* 1997; Corvaia *et al.,* 1997; Power *et al.,* 1997), it is tempting to speculate that induction of strong protective humoral responses coupled with weak or absent virus-specific cellular responses might provide the safest profile for an RSV vaccine. In conclusion, it is clear that the recombinant chimeric protein BBG2Na, comprising in part residues 130–230 of the RSV G protein, is a different immunological entity than FI-RSV or native G protein.

MATERIALS AND METHODS

Gene assembly, vector constructions, and expression of BBG2Na

Gene assembly, vector constructions, expression, and first-step protein purification of BBG2Na were undertaken as previously described (Murby *et al.,* 1995; Nguyen *et al.,* 1994). Proteins were further purified to homogeneity by reverse-phase high-performance liquid chromatography. Protein purity and antigenicity were analyzed by SDS–PAGE on 15% homogenous gels under reducing conditions and by Western blots using RSV-A-specific serum, respectively.

Virus preparation

Respiratory syncytial virus subgroup A (Long strain) was propagated in HEp-2 cells as previously described (Trudel *et al.,* 1991; Power *et al.,* 1997). Viruses were harvested after 48–72 h by scraping attached cells into the medium, centrifuging the suspension at 460 *g* for 15 min, and collecting the supernatant as the virus stock. FI-RSV was prepared as described by Prince *et al.* (1986), except that it was not concentrated by centrifugation. FI-RSV was stored at −80°C until use.

Mice

Specific pathogen-free female BALB/c mice, ages 6–9 weeks, were purchased from IFFA CREDO, l'Arbresle,

France. They were fed mouse maintenance diet AO4 (UAR, Villemoissin-sur-Orge, France) and given water *ad libitum.*

Immunization and challenge procedures

All mice were confirmed to be seronegative vis-à-vis RSV-A before inclusion in the experiments as previously described (Power *et al.,* 1997). They were immunized on days 0, 14, and 24 by intraperitoneal (i.p.) injection of 200 μl PBS solution alone or containing BBG2Na (20 μg) or FI-RSV (1/100e) in 20% $Al(OH_3)$ (Alhydrogel; vol/vol; Superfos BioSector, Vedbaek, Denmark). Seroconversion was determined 10 days following the last immunization. Mean RSV-A-specific serum antibody ELISA titers were $\log_{10}$ 5, 4, and <2, in BBG2Na-, FI-RSV-A-, and PBS-immunized mice, respectively. Mice were challenged on day 35 by i.n. instillation of 10^5 or 10^6 tissue culture infectious $doses_{50}$ RSV-A and sacrificed 2, 5, 7, 9, 12, and 14 days later.

Preparation of cells from MLN and lungs

After cardiac puncture, residual blood was removed from lung tissues by perfusion of the circulatory system with PBS containing 10 U/ml heparin. Lungs and MLN were harvested. A small fragment of lung was quick-frozen in liquid nitrogen for further RNA extraction. Lymph node cells were isolated by dissociation of MLN in RPMI 1640 (Gibco, Cergy Pontoise, France) supplemented with 15% fetal calf serum. Lungs were minced and incubated for 30 min at 37°C in an enzymatic mixture consisting type VII collagenase (75 U/ml, Sigma, St. Quentin Fallavier, France), DNase I (50 U/ml, Boehringer Mannheim Biochemica, Germany), and Dispase I (0.2 U/ml, Boehringer Mannheim Biochemica). After careful dissociation in dounce homogenizers, cell suspensions were reincubated for 30 min at 37°C, passed through a 75-μm cell strainer (Becton Dickinson, Franklin Lakes, NJ), and washed twice in RPMI 1640 with 15% fetal calf serum. Total numbers of nucleated cells were enumerated under light microscopy by the Trypan blue exclusion method (>98% viability) before preparation for flow cytometry and/or RNA extraction.

Isolation and enumeration of infiltrating eosinophils

Lung infiltrating cells were analyzed by forward and side scatter by flow cytometry (FACSvantage, Becton Dickinson, Erembodegem, Belgium) and large granular cells were sorted. Cells were centrifuged on microscopic slides (300 rpm for 3 min) (Cytospin 3, Shandon INC, Pittsburgh, PA) and stained by May-Grünwald Giemsa (Sigma). An average of 200 total cells were counted per slide to determine the percentage of eosinophils. The total number of lung infiltrating eosinophils per mouse was calculated as follows: fraction of eosinophils (light microscopy) $\times$ fraction of large granular cells (FACS) $\times$ total number of nucleated cells isolated from lungs (light microscopy).

Immunofluorescence cell staining

One hundred microliters of cells was distributed into V-bottomed 96-well plates at 3×10^5/well and centrifuged, and the pellets were washed in cold PBS. Cells were incubated at 4°C for 30 min with combinations of fluorescein, phycoerythrin, or tricolor-conjugated monoclonal antibodies to lymphocyte surface molecules CD3, CD4, CD8, CD69, CD11a/CD18 (Caltag, San Francisco, CA), TCR$\alpha\beta$ (β chain), TCR$\gamma\delta$, CD45R/B220 (Pharmingen Inc., San Diego, CA), and granulocytes (clone RB6-8C5, Caltag), at previously determined optimal concentrations. Cells were washed in cold PBS and fixed with 100 μl/well of PBS–1% paraformaldehyde. The cells were analyzed for two or three color stains using a FACScan (Becton-Dickinson) with the Lysis II software program after debris and dead cells were removed by gating on forward and side scatter. Results are expressed as means of the total number of stained cells (total number of nucleated cells $\times$ percentage of cells stained with a specific cell surface marker) $\pm$ SD obtained from parallel experiments including naive unchallenged mice and mice immunized with BBG2Na, FI-RSV, or PBS and challenged with RSV-A.

RNA extraction

Lung infiltrating cells were centrifuged at 200 *g* for 10 min, quick-frozen in liquid nitrogen, and stored at −80°C until RNA extraction. Total cellular RNA was purified by a method derived from that of Chomczynski and Sacchi (1987). Briefly, cells were lysed in RNA-B (Bioprobe Systems, Montreuil-sous-Bois, France). RNA from 3×10^5 cells was extracted with chloroform for 5 min on ice. Frozen lung fragments were weighed and disrupted in 1 ml RNA-B using a Dounce homogenizer. RNA was then extracted with chloroform from the equivalent of 1 mg lung homogenate. After centrifugation at 12,000 *g* for 15 min at 4°C, RNA in the aqueous phase was precipitated with 1 vol isopropanol and washed with 75% ethanol. The RNA pellet was resuspended in 100 μl diethylpyrocarbonate-treated water; 2.5 μl was subjected to PCR analysis to exclude genomic DNA contamination. An additional precipitation of the RNA was performed with 2 vol of ethanol in the presence of 0.2 M NaCl. Average yields were approximately 1 μg total RNA. Purified RNA was stored at −80°C until reverse transcribed.

Primers and probes

Primers and probes were synthesized by Genset SA (Paris, France) and are shown in Table 1. Sequences were obtained from Clontech Laboratories (Ozyme, Paris, France) or Stratagene (LaJolla, CA) or were based on published sequences. Oligonucleotides specific for

TABLE 1

Oligonucleotide Sequences and Reaction Conditions Used in mRNA cDNA Detection by RT-PCR–ELISA

Gene	Primer sequence	Probe sequence	PCR product size (bp)	Number of PCR cycles
Genomic DNA	(+) 5′-GTGGGCCGCTCTAGGCACCAA-3′[a] (−) 5′-CTCTTTGATGTCACGCACGATTTC-3′[a]	—	540	35
β-Actin	(+) 5′-TGTGATGGTGGGAATGGGTCAG-3′[b] (−) 5′-TTTGATGTCACGCACGATTTCC-3′[b]	(+) 5′-(b)AGCAAGAGAGGTACTCT-3′[d]	514	26
IL-2	(+) 5′-GTCAACAGCGCACCCACTTCAAGC-3′[b] (−) 5′-GCTTGTTGAGATGATGCTTTGACA-3′[b]	(−) 5′-(b)GTTCATCTTCTAGGCACTG-3′[c]	450	30
IL-4	(+) 5′-CCAGCTAGTTGTCATCCTGCTCTTCTTTCTCG-3′[a] (−) 5′-CAGTGATGTGGACTTGGACTCATTCATGGTGC-3′[a]	(+) 5′-(b)ACGGAGATGGATGTGCCAAACTC-3′[b]	357	30
IL-5	(+) 5′-ATGAGAAGGATGCTTCTGCACTTGA-3′[a] (−) 5′-GTCACCATGGAGCAGCTCAGCC-3′[a]	(−) 5′-(b)GCCTTCCATTGCCCACTCTGTAC-3′[b]	425	30
IL-10	(+) 5′-GTGAAGACTTTCTTTCAAACAAAG-3′[b] (−) 5′-CTGCTCCACTGCCTTGCTCTTATT-3′[b]	(+) 5′-(b)ATGCAGGACTTTAAGGGTTACTTGGGTT-3′[a]	274	30
IL-13	(+) 5′-TCTCCCCAGCAAAGTCTGAT-3′[c] (−) 5′-CTGGATTCCCTGACCAACAT-3′[c]	(−) 5′-(b)GGTCTCCCAGCCTCCCCGATA-3′[c]	262	30
IFN-γ	(+) 5′-TACTGCCACGGCACAGTCATTGAA-3′[b] (−) 5′-GCAGCGACTCCTTTTCCGCTTCCT-3′[b]	(−) 5′-(b)TGGACCTGTGGGTTGTTGACCTCAAACTTGGC-3′[a]	405	30
RSV-A G	(+) 5′-CTTCAACAACACCAGGAGTC-3′[e] (−) 5′-TGGTGTTGATGGTTGGCTC-3′[e]	(+) 5′-(b)GCAACAATCCAACCTGCTGGG-3′[e]	369	35

[a] Sequences obtained from Clonetech.
[b] Sequences obtained from Stratagene.
[c] Sequences obtained from Warris *et al.,* 1996.
[d] Sequences obtained from Montgomery *et al.,* 1991.
[e] Sequences determined according to Wertz *et al.,* 1985.

the RSV-A G gene were determined using the MacVector software program (Oxford Molecular Group, Oxford, UK). For PCR amplification, primer concentrations were 0.8 μM for genomic DNA, IL-4, IL-5, and RSV-A G cDNAs and 1 μM for β-actin, IL-2, IL-10, IL-13, and IFN-γ cDNAs. Products span intron–exon junctions, thereby ensuring a cytokine mRNA-derived PCR product. In the semiquantitative ELISA protocol, 5′ biotinylated oligonucleotide probes were 15 and 25 pmol/ml hybridization solution for IL-5 and IL-13, respectively, and 7.5 pmol/ml for all other PCR products.

RT-PCR ELISA detection of mRNA

The isolated RNA was first reverse transcribed to cDNA with 1 μg oligo(dT)15 (Promega, Lyon, France) and 15 U AMV reverse transcriptase (Promega) in a final volume of 35 μl, according to the manufacturer's instructions. The cDNA library was then diluted twofold with sterile water and stored at −20°C until required. For PCRs, 2 μl of cDNA was added to 23 μl of standard PCR buffer (Perkin–Elmer, Roissy, France) supplemented with 5% LB broth and containing unlabeled dNTPs (200 μM each) plus 10 μM digoxigenin (DIG)-labeled dUTP (Boehringer Mannheim, Meylan, France) and 2.5 U of AmpliTaq Gold DNA polymerase (Perkin–Elmer). For IL-13, buffer conditions were Tris–HCl, pH 8.6, and 2.5 mM $MgCl_2$. The sequence of PCR amplification consisted of a first step at 95°C for 10 min, followed by 30 cycles at 15 s at 95°C, 1 min at 60°C (55°C for RSV-specific primers), and 1 min at 72°C. The amplification was terminated by a final extension step at 72°C for 7 min. Amplifications were performed in a Perkin–Elmer 9600 or 9700 thermal cycler. β-Actin cDNA was amplified as an internal control for variations in RNA extractions and cDNA synthesis. β-Actin cDNAs were of comparable levels for all samples analyzed. The linear range of signal strength was determined by performing titration for cDNA and cycle numbers to obtain nonsaturated PCRs for each amplification. Negative and positive controls consisted of amplifications with water instead of cDNA and with saturating amounts of gel-purified specific PCR product, respectively.

PCR products were first checked for appropriate size in 2% agarose gels containing ethidium bromide. Subsequently, amplicon identities were confirmed and quantified by a semiquantitative ELISA protocol (Boehringer Mannheim). Briefly, 2.5 μl of the amplified product (pure or 1:10 or 1:50 dilutions) was incubated with 20 μl of denaturation solution for 10 min, followed by addition of 225 μl of hybridization buffer containing the specific biotinylated oligonucleotide probe. Controls included the negative and positive PCR samples, a control DIG-labeled product, and a specific probe provided by the manufacturer. Two hundred microliters of the solution was distributed in a multiwell streptavidin-coated plate and incubated under agitation at 37°C for 3 h. The plate was then washed and any bound product was detected with peroxidase-conjugated anti-DIG antibodies in a

standard colorimetric reaction using 2′-azino-di[3-ethylbenthiazoline sulfonic acid] substrate. The OD_{405nm} was recorded. Under these conditions, the OD_{405nm} was directly proportional to the level of target PCR product, which was subsequently normalized relative to OD_{405nm} detected for β-actin mRNA.

Statistical analyses

Statistical analyses were done using the multirange and *t* test of the Statgraphic software program (Manugistics, Rockville, MD).

ACKNOWLEDGMENTS

H.P.G. and T.H. contributed equally to the completion of this work. We thank Dominique Cyblat, Francis Derouet, Vincent Michaud, Fabienne Damien, and Franck Gueneau for expert technical help. We are also grateful to Professor J.-P. Revillard, Dr. C. Czerkinsky, Dr. L. Chevalet, and Dr. A. Robert for advice and expertise. We thank Dr. N. Corvaïa for critically reviewing the manuscript.

REFERENCES

Alwan, W. H., Kozlowska, W. J., and Openshaw, P. J. (1994). Distinct types of lung disease caused by functional subsets of antiviral T cells. *J. Exp. Med.* **179,** 81–89.

Anderson, L. J., and Heilman, C. A. (1995). Protective and disease-enhancing immune responses to respiratory syncytial virus. *J. Infect. Dis.* **171,** 1–7.

Anderson, L. J., Norden, J., Saunders, D., Toms, G. L., and Scott, R. (1990). Analysis of the local and systemic immune responses induced in BALB/c mice by experimental respiratory syncytial virus infection. *J. Gen. Virol.* **71,** 1561–1570.

Anderson, L. J., Tsou, C., Potter, C., Keyserling, H. L., Smith, T. F., Ananaba, G., and Bangham, C. R. (1994). Cytokine response to respiratory syncytial virus stimulation of human peripheral blood mononuclear cells. *J. Infect. Dis.* **170,** 1201–1208.

Barrera, J. C., and Letchworth, G. J. (1996). Persistence of vesicular stomatitis virus New Jersey RNA in convalescent hamsters. *Virology* **219,** 453–464.

Brandt, C., Power, U. F., Plotnicky-Gilquin, H., Huss, T., Nguyen, T., Lambert, P-H., Binz, H., and Siegrist, C-A. (1977). Protective immunity against respiratory syncytial virus in early life following murine maternal or neonatal vaccination with the recombinant G fusion protein BBG2Na. *J. Infect. Dis.* **176,** 884–891.

Cane, P. A., Mattews, D. A., and Pringle, C. R. (1991). Identification of variable domains of the attachment (G) protein of subgroup A respiratory syncytial viruses. *J. Gen. Virol.* **72,** 2091–2096.

Chomczynski, P., and Sacchi, N. (1987). Single-step method of RNA isolation by acid guanidinium thiocyanate–phenol–chloroform extraction. *Anal. Biochem.* **162,** 156–159.

Collins, P. L., McIntosh, K., and Chanock, R. M. (1996). Respiratory syncytial virus. *In* "Fields Virology" (D. M. Knipe and P. M. Howley, Eds.), pp. 1313–1351. Lippincott–Raven, Philadelphia.

Connors, M., Collins, P. L., Firestone, C. Y., and Murphy, B. R. (1991). Respiratory syncytial virus (RSV) F, G, M2 (22K), and N proteins each induce resistance to RSV challenge, but resistance induced by M2 and N proteins is relatively short-lived. *J. Virol.* **65,** 1634–1637.

Connors, M., Kulkarni, A. B., Firestone, C.-Y., Holmes, K. L., Morse, H. C., III, Sotnikov, A. V., and Murphy, B. R. (1992). Pulmonary histopathology induced by respiratory syncytial virus (RSV) challenge of formalin-inactivated RSV-immunized BALB/c mice is abrogated by depletion of CD4+ cells. *J. Virol.* **66,** 7444–7451.

Connors, M., Giese, N. A., Kulkarni, A. B., Firestone, C.-Y., Morse, H. C., and Murphy, B. R. (1994). Enhanced pulmonary histopathology induced by respiratory syncytial virus (RSV) challenge of formalin-inactivated RSV-immunized BALB/c mice is abrogated by depletion of interleukin-4 (IL-4) and IL-10. *J. Virol.* **68,** 5321–5325.

Corvaia, N., Tournier, P., Nguyen, T. N., Haeuw, J. F., Power, U. F., Binz, H., and Andréoni, C. (1997). Challenge of BALB/c mice with respiratory syncytial virus does not enhance the Th2 pathway induced after immunization with a recombinant G fusion protein, BBG2Na, in aluminum hydroxide. *J. Infect. Dis.* **176,** 560–569.

Fiorentino, D. F., Zlotnik, A., Mosmann, T. R., Howard, M., and Garra, A. O. (1991). IL-10 inhibits cytokine production by activated macrophages. *J. Immunol.* **147,** 3815–3822.

Graham, B. S., Henderson, G. S., Tang, Y.-W., Lu, X., Neuzil, K. M., and Colley, D. G. (1993). Priming immunization determines T helper cytokine mRNA expression patterns in lungs of mice challenged with respiratory syncytial virus. *J. Immunol.* **151,** 2032–2040.

Hancock, G. E., Speelman, D. J., Heers, K., Bortell, E., Smith, J., and Cosco, C. (1996). Generation of atypical pulmonary inflammatory responses in BALB/c mice after immunization with the native attachment (G) glycoprotein of respiratory syncytial virus. *J. Virol.* **70,** 7783–7791.

Hegele, R. G., Hayashi, S., Bramley, A. M., and Hogg, J. C. (1994). Persistence of respiratory syncytial virus genome and protein after acute bronchiolitis in guinea pigs. *Chest* **105,** 1848–1854.

Hussell, T., Spender, L. C., Georgiou, A., O Garra, A., and Openshaw, P. J. (1996). Th1 and Th2 cytokine induction in pulmonary T cells during infection with respiratory syncytial virus. *J. Gen. Virol.* **77,** 2447–2455.

Janezic, A., Semper, A., Holloway, J., and Holgate, S. (1995). Detection of cytokine mRNA expression by a sensitive RT-PCR ELISA detection system. *Biochemica* **3,** 30–32.

Johnson, P. R., and Collins, P. L. (1988). The A and B subgroups of human respiratory syncytial virus: Comparison of intergenic and gene-overlap sequences. *J. Gen. Virol.* **69,** 2901–2906.

Kim, H. W., Canchola, J. G., Brandt, C. D., Pyles, G., Chanock, R. M., Jensen, K., and Parrott, R. H. (1969). Respiratory syncytial virus disease in infants despite prior administration of antigenic inactivated vaccine. *Am. J. Epidemiol.* **89,** 422–434.

Libon, C., Corvaia, N., Haeuw, J. F., Nguyen, T. N., Ståhl, S., Bonnefoy, J.-Y., and Andréoni, C. (1999). The serum albumin-binding region of streptococcal protein G (BB) potentiates the immunogenicity of the G130–230 RSV-A protein. *Vaccine* **17,** 406–414.

Makrides, S. C., Nygren, P. A., Andrews, B., Ford, P. J., Evans, K. S., Hayman, E. G., Adari, H., Uhlen, M., and Toth, C. A. (1996). Extended in vivo half-life of human soluble complement receptor type 1 fused to a serum albumin-binding receptor. *J. Pharmacol. Exp. Ther.* **277,** 534–542.

Montgomery, R. A., and Dallman, M. J. (1991). Analysis of cytokine gene expression during fetal thymic ontogeny using the polymerase chain reaction. *J. Immunol.* **147,** 554–560.

Murby, M., Samuelsson, E., Nguyen, T. N., Mignard, L., Power, U., Binz, H., Uhlen, M., and Stahl, S. (1995). Hydrophobicity engineering to increase solubility and stability of a recombinant protein from respiratory syncytial virus. *Eur. J. Biochem.* **230,** 38–44.

Murphy, B. R., Hall, S. L., Kulkarni, A. B., Crowe, J. E., Jr., Collins, P. L., Connors, M., Karron, R. A., and Chanock, R. M. (1994). An update on approaches to the development of respiratory syncytial virus (RSV) and parainfluenza virus type 3 (PIV3) vaccines. *Virus Res.* **32,** 13–36.

Murphy, B. R., Sotnikov, A., Lawrence, L. A., Banks, S. M., and Prince, G. A. (1990). Enhanced pulmonary histopathology is observed in cotton rats immunized with formalin-inactivated respiratory syncytial virus (RSV) or purified F glycoprotein and challenged with RSV 3–6 months after immunization. *Vaccine* **8,** 497–502.

Nguyen, T. N., Uhlén, M., and Ståhl, S. (1994). De novo gene assembly using a paramagnetic solid support. *In* "Advances in Biomagnetic Separation" (M. Uhlén, E. Hornes, and O. Olsvik, Eds.), pp. 73–78. Eaton, Natick.

Nygren, P. À., Flodby, P., Andersson, R., Wigzell, H., and Uhlen, M. (1991). In vivo stabilization of a human recombinant CD4 derivative by

fusion to a serum albumin-binding receptor. *In* "Vaccines 91, Modern Approaches to Vaccine Development" (R. M. Chanock, F. Brown, H. S. Ginsberg, and R. A. Lerner, Eds.), pp. 363–368. Cold Spring Harbor Laboratory Press, Cold Spring Harbor, NY.

Openshaw, P. J. M. (1991). Pulmonary epithelial T cells induced by viral infection express T cell receptors alpha/beta. *Eur. J. Immunol.* **21,** 803–806.

Openshaw, P. J. M., Anderson, K., Wertz, G. W., and Askonas, B. A. (1990). The 22-kilodalton protein of respiratory syncytial virus is a major target for K^d-restricted cytotoxic T lymphocytes from mice primed by infection. *J. Virol.* **64,** 1683–1689.

Power, U. F., Plotnicky-Gilquin, H., Huss, T., Robert, A., Trudel, M., Stahl, S., Uhlen, M., Nguyen, T. N., and Binz, H. (1997). Induction of protective immunity in rodents by vaccination with a prokaryotically expressed recombinant fusion protein containing a respiratory syncytial virus G protein fragment. *Virology* **230,** 155–166.

Prince, G. A., Jenson, A. B., Hemming, V. G., Murphy, B. R., Walsh, E. E., Horswood, R. L., and Chanock, R. M. (1986). Enhancement of respiratory syncytial virus pulmonary pathology in cotton rats by prior intramuscular inoculation of formalin-inactivated virus. *J. Virol.* **57,** 721–728.

Routledge, E. G., Willcocks, M. M., Samson, A. C., Morgan, L., Scott, R., Anderson, J. J., and Toms, G. L. (1988). The purification of four respiratory syncytial virus proteins as protective agents against experimental infection in BALB/c mice. *J. Gen. Virol.* **69,** 293–303.

Sparer, T. E., Matthews, S., Hussel, T., Rae, A. J., Garcia-Barreno, B., Melero, J. A., and Openshaw, P. J. (1998). Eliminating a region of respiratory syncytial virus attachment protein allows induction of protective immunity without vaccine-enhanced lung eosinophilia. *J. Exp. Med.* **187,** 1921–1926.

Stott, E. J., Taylor, G., Ball, L. A., Anderson, K., Young, K. K., King, A. M., and Wertz, G. W. (1987). Immune and histopathological responses in animals vaccinated with recombinant vaccinia viruses that express individual genes of human respiratory syncytial virus. *J. Virol.* **61,** 3855–3861.

Swain, S. L. (1991). Lymphokines and the immune response: The central role of interleukin-2. *Curr. Opin. Immunol.* **3,** 304–310.

Taylor, G., Stott, E. J., and Hayle, A. J. (1985). Cytotoxic lymphocytes in the lungs of mice infected with respiratory syncytial virus. *J. Gen. Virol.* **66,** 2533–2538.

Tebbey, P. W., Hagen, M., and Hancock, G. E. (1998). Atypical pulmonary eosinophilia is mediated by a specific amino acid sequence of the attachment (G) protein of respiratory syncytial virus. *J. Exp. Med.* **10,** 1967–1972.

Trudel, M., Nadon, F., Seguin, C., and Binz, H. (1991). Protection of BALB/c mice from respiratory syncytial virus infection by immunization with a synthetic peptide derived from the G glycoprotein. *Virology* **185,** 749–757.

Vaux-Peretz, F., Chapsal, J. M., and Meignier, B. (1992). Comparison of the ability of formalin-inactivated respiratory syncytial virus, immunopurified F, G and N proteins and cell lysate to enhance pulmonary changes in Balb/c mice. *Vaccine* **10,** 113–118.

Waris, M. E., Tsou, C., Erdman, D. D., Day, D. B., and Anderson, L. J. (1997). Priming with live respiratory syncytial virus (RSV) prevents the enhanced pulmonary inflammatory response seen after RSV challenge of BALB/c mice immunized with formalin-inactivated RSV. *J. Virol.* **71,** 6935–6939.

Waris, M. E., Tsou, C., Erdman, D. D., Zaki, S. R., and Anderson, L. J. (1996). Respiratory syncytial virus infection in BALB/c mice previously immunized with formalin-inactivated virus induces enhanced pulmonary inflammatory response with a predominant Th2-like cytokine pattern. *J. Virol.* **70,** 2852–2860.

Wertz, G. W., Collins, P. L., Huang, Y., Gruker, C., Levine, S., and Ball, L. A. (1985). Nucleotide sequence of the G protein gene of human respiratory syncytial virus reveals an unusual type of viral membrane protein. *Proc. Natl. Acad. Sci. USA* **82,** 4075–4079.